

# Magnetic Zeppelin: Detection of gravitational drive in the Hz regime

Tim M. Fuchs<sup>1</sup>, Dennis Uitenbroek<sup>1</sup>, Jaimy Plugge<sup>1</sup>, Noud van Halteren<sup>1</sup>, Andrea Vinante<sup>3</sup>, Hendrik Ulbricht<sup>2</sup> and Tjerk H. Oosterkamp<sup>1\*</sup>

<sup>1</sup>Leiden Institute of Physics, Leiden University, P.O. Box 9504, 2300 RA Leiden, The Netherlands.

<sup>2</sup>School of Physics and Astronomy, University of Southampton, SO17 1BJ, Southampton, UK.

<sup>3</sup>Istituto di Fotonica e Nanotecnologie, CNR and Fondazione Bruno Kessler, I-38123 Povo, Trento, Italy.

\*Corresponding author(s). E-mail(s): [oosterkamp@physics.leidenuniv.nl](mailto:oosterkamp@physics.leidenuniv.nl);

## Abstract

Extremely isolated mechanical resonators are excellent probes for small scale forces and quantum mechanical effects. Furthermore, such systems operating at low frequencies and appreciable mass are well suited to measure both quantum mechanical effects, and gravitational effect, whose exact descriptions have yet to be unified. In this paper we demonstrate a sub-millimeter scale magnetic particle, levitated inside a type-I superconducting trap. At a frequency of 26.7 Hz, a mass of 0.4 mg and showing Q-factors in excess of  $10^7$ , we obtained a force noise of  $0.5 \text{ fN}\sqrt{\text{Hz}}$ . This force sensitivity was then validated by driving the magnetic particle using a time varying gravitational gradient supplied by brass masses on an electric wheel positioned underneath the cryostat, paving the way for future experiments gravitationally coupling small test and source masses. We measured a signal at  $3/8$  of the expected Newtonian gravitational force at the location of the magnetic particle. We attribute this difference to the effect of the gravitational drive on the mass spring system from which the trap was suspended. This work provides a stepping stone towards mesoscopic probes of gravity and the quantum nature of gravity, and can find application in magnetometry and magnetic resonance force microscopy.

# 1 Introduction

Extremely soft micromechanical resonators can be used for the mechanical sensing of very weak signals and to probe quantum physics at increasing scales of mass and space. The extremely low damping of these systems, and consequently their low coupling to the environment, makes them well suited for mesoscopic probes of quantum mechanics and could provide a test to possible limits of the applicability of quantum mechanics to the macroscopic world [1, 2]. The extremely soft coupling and resulting high isolation from the environment are critical to any quantum mechanical experiment at low frequency, since even at mK temperatures the bath temperature will otherwise dominate the decoherence time of any quantum state. These systems are especially suited for tests in a regime with appreciable gravitational influences, which is favourable in probing [3, 4] physical models of the wave function collapse [5], namely those that feature the system mass explicitly, such as the continuous spontaneous localization (CSL) model [6] and the Diósi-Penrose model of gravitationally-induced collapse [7–9].

In a recent publication, the group of Markus Aspelmeyer has demonstrated gravitational coupling between two 90 mg, 1 mm radius, gold spheres, achieved off resonance at mHz frequencies [10]. Recent work by Brack et al. [11] has shown the dynamical detection of gravitational coupling between two meter sized parallel beams at 20 hertz. In this paper we present work with a 2.4 kg source mass and a sub-milligram test mass as an intermediate step where a small test mass senses the gravity sourced by a small source mass. We perform the experiment at 26.7 Hz, where the main problem was to get back-ground vibration levels sufficiently low.

Furthermore, in following of Bob van Waarde[12], Vinante et al. [13] have demonstrated that magnetically levitated particles can be used as resonators with extremely low damping and thus very high Q factors. Their motion can be detected using SQUID detection of the change in flux in a nearby coil due to the particles motion at frequencies in the range of 1-100 Hz. Because the particles are levitated above a type-I superconductor, the experiments are performed at cryogenic temperatures of 4 Kelvin. Together with the low damping this results in a very low force noise. These superconducting traps also provide excellent shielding from magnetic and electric forces, further shielding the probe from non-gravitational sources of noise. This, then, seems to be a promising route for combining millimeter sized test masses with detection in the hertz regime.

In this paper we present our work to push these levitated micromagnets into the regime of detecting very small (gravitational) forces. We discuss a levitated magnetic zeppelin with  $m_{\text{particle}} = 0.43$  mg, confined in a cylindrical elliptical tantalum trap with height 5.5 mm and principal axes of 4.5 and 3.5 mm. We perform our measurements at mK temperatures in a cryogen-free dilution-refrigerator with multi-stage vibration isolation to reduce the force noise of our resonator.

To demonstrate our force sensitivity and validate the magnetic zeppelin's feasibility as a gravitational test mass, we have excited a translational degree

of freedom of our levitated zeppelin by applying a time varying gravitational gradient. Further work must recast the magnetic zeppelin as a gravitational source mass.

## 2 Experimental setup

The core of the set-up is a type-I superconducting trap with a magnetic zeppelin levitated therein, as shown in Fig. 1b. The trap is made of Tantalum with a critical temperature of  $T_c = 4.48$  K. We perform the experiment at temperatures below 100 mK. The trap has an elliptical shape to confine the modes of the levitated magnetic zeppelin to the axis system of the trap and to provide each of the six degrees of freedom with a well defined resonant frequencies. By choosing proper dimensions all six resonant frequencies sufficiently high to bring them well within the range of frequencies where the vibration isolation works well. The 'rigid air-frame' of the zeppelin, that provides the lift, is constructed out of a set of three  $0.25 \text{ mm} \times 0.25 \text{ mm} \times 0.25 \text{ mm}$   $\text{Nd}_2\text{Fe}_{14}\text{B}$  magnets that are magnetically attached North-to-South as also shown in Fig. 1b. Typical remnant magnetisation of magnets of this type is in the order of 1.4 T. The 'gondola' consists of a spherical glass bead with a 0.25 mm radius and is attached to the middle magnet using Stycast. This gondola is attached in an effort to break the rotational symmetry of the zeppelin around the x-axis (angle  $\gamma$ ). The estimated mass of the full zeppelin, as depicted in Fig. 1d., is 0.43 mg.

The motion of the zeppelin results in a change of flux through a loop at the top of the trap (the pick-up loop). We place the loop off center so that the symmetry is broken, and all modes couple to the loop. The flux change due to motion of rotation of the zeppelin is then detected using a two-stage biased SQUID coupled inductively to the pick-up loop. A third loop made halfway between the SQUID Input loop and the pick-up loop is coupled inductively to a Calibration loop. This transformer is used to calibrate the energy coupling  $\beta^2$  between the detection circuit and the degrees of motion of the zeppelin. This procedure is further described in App. C.

The entire set-up is hung by springs from a multi-stage mass spring system to shield the experiment from external vibrations, both vertical and lateral. The bottom three masses (one aluminum, two copper) are similar in weight to the experimental set-up, with a lowest resonance frequency at 0.9 Hz. Above that is a mK mass spring system with a lowest resonance frequency of 4.8 Hz. We refer to Ref. [14] for more details on a near identical mass-spring system and its performance in a similar dilution refrigerator. This combination is hung from the Still plate by a long spring. Thermalization of the experiment is provided by a flattened silver wire, which is mechanically soft but provides a good thermal link. This entire system, sometimes referred to as our 'Christmas tree', is depicted in Fig. 1a.

The cryostat as a whole is attached to a 25 metric ton concrete block, which is again placed on pneumatic dampers to limit vibrations coupling in from the

building. The pulse tube cooler and the vacuum pumps for the circulation of the mixture are rigidly attached to the building through a second frame, and attached to the cryostat only by edge welded bellows and soft copper braiding.

In an effort to further demonstrate the force sensitivity of the system and as a proof of concept for gravitational detection by means of these levitated zeppelins, we utilized a electric bike wheel with a set of three 2.45 kg brass masses placed equally spaced along the outer rim. This wheel was used to create a time dependent gravitational gradient at the resonant frequency of a select mode of the zeppelin, in an effort to drive the motion gravitationally. The frequency of the masses was read-out using a simple laser and optical detector combination, in which the masses act as a mechanical shutter.

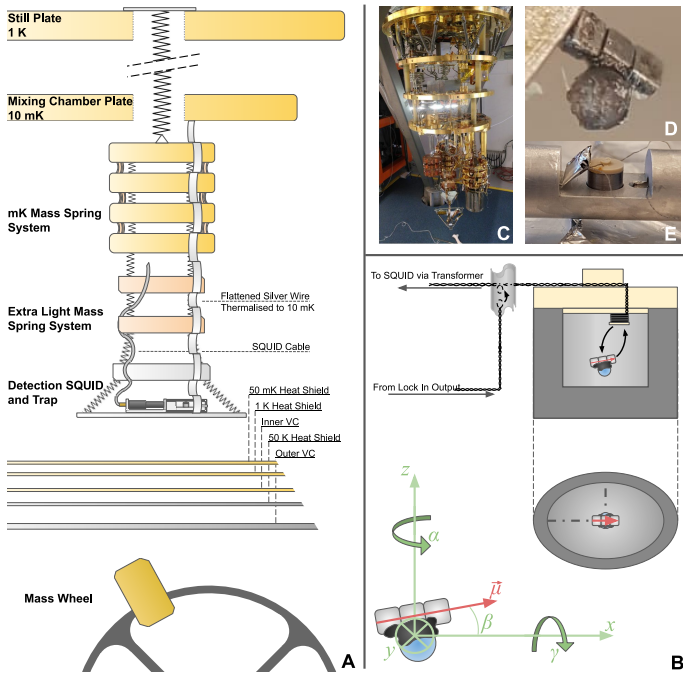


**Fig. 1:** Schematic depiction of the experimental setup. **A:** Magnetic shielding of the Tantalum trap using Mu-metal strips and an aluminium holder in the superconducting state. Magnetic shielding of the detection SQUID (Magnicon CAR-1 Two Stage SQUID) by Niobium can (Magnicon NC-1). The experiment is suspended from a multi-stage mass spring system to isolate from external vibrations. **B:** Conventions for degrees of freedom adopted from Vinante et al. [13]. Particle motion is confined to the axial system of the holder by breaking the symmetry of the trap. Zeppelin motion is picked-up by a superconducting coil placed off-center with respect to the trap (pick-up (PU) loop) and detected using the SQUID. PU-loop and SQUID are connected by superconducting twisted pair and niobium screw terminals on the SQUID input coil. Inside the magnetic shielding around the trap, a small coil is coupled inductively to a single loop made in one of the cables connecting the PU-loop to the input coil of the SQUID (Calibration Transformer). This transformer allows for absolute calibration of the particle motion. **C, D, E:** An image of the dilution fridge used for the experiments, including the multi-stage mass spring system; the magnetic zeppelin, made up out of three 0.25 mm x 0.25 mm x 0.25 mm  $\text{Nd}_2\text{Fe}_{14}\text{B}$  magnets (SuperMagnetMan, C0005-10) magnetically attached end-to-end and a single spherical glass bead with a 0.25 mm radius attached using Stycast to the middle of the magnets, which is used to break the symmetry of the  $\gamma$  mode; The trap as placed in the aluminium holder without the shielding cylinder. The aluminium foil envelope provides additional shielding between the calibration transformer and the PU-loop. Further details and images of the setup are shown in Appendix A.

### 3 Results

In figure 2B, we show the uncalibrated spectrum as measured for our run during which we measured our gravitational drive. We clearly observe the 6 different modes corresponding to the three translational modes, and rotational modes respectively. These modes were validated and calibrated by performing a magnetic drive, excited by a flux injected through the calibration transformer, as shown in figure 1B.

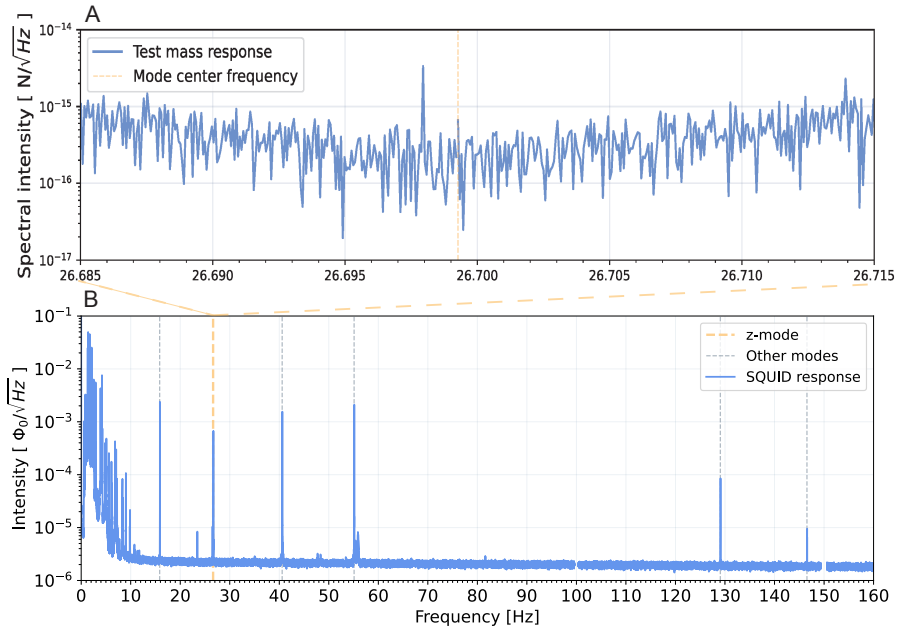


**Fig. 2:** *A:* Force Noise of the 26 Hz Mode when gravitationally driven at 1.3 mHz detuning, overnight. *B:* Typical zeppelin power spectrum. In this figure we have left out the regular 50Hz european electrical noise. Which typically has a similar power to the zeppelin resonances.

Using this magnetic drive, we determine the decay time of the modes during the subsequent ringdown. For the 26.7 Hz mode, we find a lower bound  $\tau = 1.09 \cdot 10^5$  s, or a Q factor of  $Q = 9.13 \cdot 10^6$ . This procedure is further discussed in appendix B. For the other modes we arrive at Q factors that are about an order of magnitude lower.

We demonstrate the force sensitivity of our mode, and test for future gravitational coupling between two trapped particles by driving the 26.7 Hz mode using the brass masses of the mass-wheel. The resulting excitation at one position of the wheel in the force spectrum is shown in figure 2A. The calibration of this spectrum is discussed in appendix B, C, D. The resulting force noise

of this z-mode is approximately  $0.3 \text{ fN}/\sqrt{\text{Hz}}$  in an 8 mHz bandwidth centered around the orange dotted line that indicates the frequency of the resonance. This value varies from one night to the next.

Equivalently, we can determine the motion of the trap in which the zeppelin is levitated by dividing the force noise by the spring constant of the confinement potential that keeps the zeppelin around its equilibrium height. The spring constant for this z-mode is  $k = 12.2 \cdot 10^{-3}$ , resulting in a trap displacement noise of  $30 \text{ fm}/\sqrt{\text{Hz}}$ . This vibrational noise of the experiment is exceptionally low, but still causes the motion of the zeppelin to be excited more than one would expect for its thermal motion. This corresponds to a mode temperature of 3 K, which we attribute to the limits of the vibration isolation inside the cryostat at the time of the experiment for such a high Q factor. It would require another 20dB of vibration isolation to reach thermal motion at 30 mK. Please note that for white excitation noise the mode temperature scales with the square root of the Q factor. If, in the future, the Q factors increase further, even more vibration isolation is required to continue towards lower force noise.

In figure 3 we show the level of this excitation peak for different displacements of the wheel. We also show the phase response of the particle with respect to the reference phase of a mass passing the highest point along its trajectory. Included is the expected gravitational signal at the location of the magnetic zeppelin for the z-mode of the zeppelin, which was taken from analytical simulation for point masses.

We observe an agreement in the amplitude to a factor 3/8. We attribute this constant factor to the effect of the wheel on the trap. Since the centre of mass of the trap and the holder are closely spaced, they both experience a similar gravitational gradient. This force will cause a reduction in the gravitational response of the zeppelin, since the trap response is far above resonance of the vibration isolation system, which in turn leads to a  $180^\circ$  phase shift. The resulting motion of the trap then leads to a damping of the effective response of the zeppelin.

## 4 Conclusions

By ensuring that the pick-up loop is placed off-centre with respect to the trap and by breaking the rotational symmetry in  $\gamma$  we demonstrate detection of all six modes, in comparison to earlier work. As we will discuss in future work, this is critical to the stability of the mode under test due to non-linear mixing between the different modes.

We demonstrate the detection of a 30 aN gravitational signal at 26 Hz and a damping linewidth as low as  $\gamma/2\pi = 2.92 \mu\text{Hz}$ , with a 0.43 mg test mass, paving the way for future experiments in which both source and test mass are in this regime. This work could already provide a more stringent bound on dissipative collapse models. Furthermore it provides a promising platform to test fifth force models, MOND theories and other extensions of the standard model.

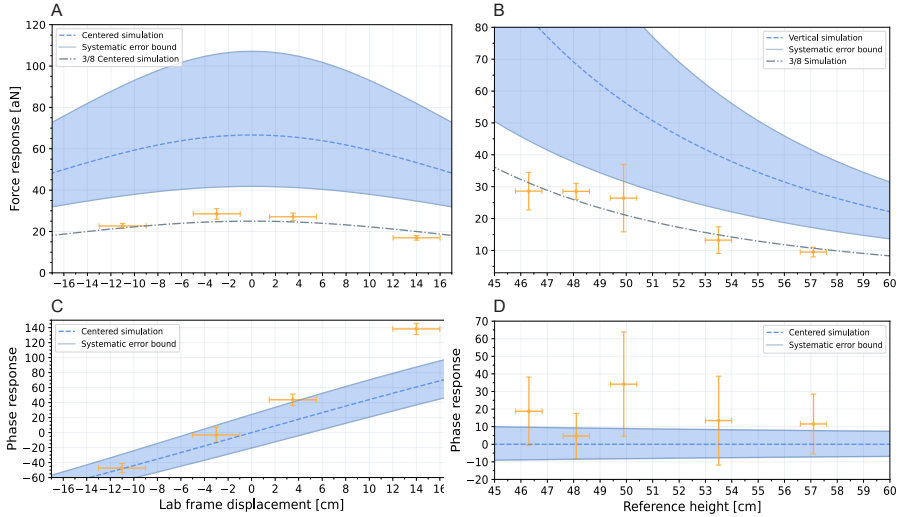


**Fig. 3:** *A:* Force measured by the zeppelin as a result from drive using the mass wheel, for different lateral displacement of the mass wheel relative to the zeppelin. The solid line represents the simulated gravitational force at the position of the zeppelin as a function of the lateral displacement of the mass wheel. A second, dashed line is plotted, which has a scaling factor of 2.5 applied, that seems to agree with the data more closely. *B:* Similar to *A*, but now for a vertical displacement of the mass wheel relative to the zeppelin *C:* Here we see the phase response of the zeppelin relative to the drive of the mass wheel for different lateral positions of the mass wheel. *D:* Similar to *C*, but now for a vertical displacement.

By using a second zeppelin in a different trap as source mass, or a similar construction, this work paves the way towards easily scalable measurements of gravitational coupling in the Hz regime. Coupling of the detection SQUIDs in this scheme to an LC circuit would provide a means of inserting microwave photons, providing access to the optical toolbox of quantum state manipulation. This would further extend this work towards truly macroscopic superposition measurements and gravitationally-induced entanglement.

**Acknowledgments.** We acknowledge support from EU EIC project QuCom and support from the NWO grant OCENW.GROOT.2019.088. We thank K. Heeck, P. Numberi, G. Koning and M. Camp for useful discussions and experimental help.

## Appendix A Further Schematics and Photographs of the Setup

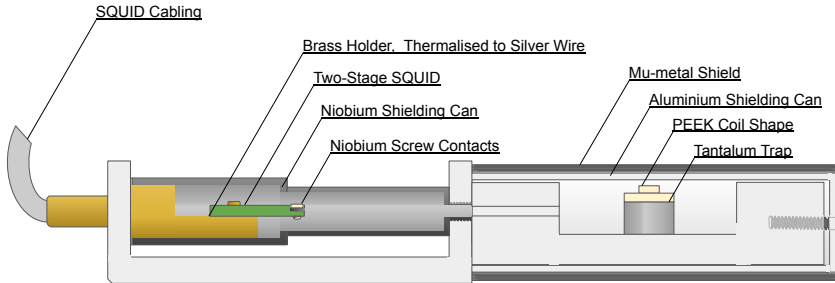


**Fig. A1:** Close-up of the experiment holder in Fig. 1. The SQUID detection chip is housed in a niobium can (respectively, Magnicon CAR-1 Two-Stage SQUID and NC-1 Can) that provides shielding from AC magnetic fields through the Meissner effect. The niobium can is screwed into the larger aluminium holder, which similarly provides AC magnetic shielding to the trap. The tantalum trap is capped with a PEEK coil-shape, placed offset from the center of the trap, around which the pick-up loop is wound. Additional shielding from DC magnetic fields is provided by several layers of Mu-metal foil wrapped around the aluminium holder. This shielding was added under the assumption that stray magnetic fields influence the position of the zeppelin within the trap and get 'frozen-in' to the superconductors as they cool down.





**Fig. A2:** Photos of the the experimental apparatus of Fig. 1. a. The mass-spring system and the silver wire used for thermalisation of the masses and the experiment, with at the bottom the holder on a small triangular platform to attach the springs. b. The coil after two layers of 5 loops were wound around it, with the rest of the cap above. The final pick-up loop consisted of four layers. c. A close-up of the calibration transformer, before aluminium shielding was added around it. d. The tantalum trap, with the oval shape and milling marks visible. e. The 'mass-wheel' as used in the experiments to show gravitational coupling. The three brass masses are placed in an equilateral triangle. Not shown is the laser pen-detector combination used to read out the frequency of the masses. The wheel is surrounded with one centimeter thick steel plates and is attached to a bridge made out of MK-profiles, which is used to control the elevation and positioning of the wheel in the lab relative to the trap inside the cryostat.

## Appendix B Determination of decay time, damping factor, and the quality factor of the mechanical modes

The exponential decay time  $\tau$  of each mode was determined through ringdown measurements at high amplitude. We focus on the 26 Hz mode, since this is the mode we used to detect our gravitational signal, as it displayed the highest level of vibrational isolation when driven through external seismic vibrations. We suspect it to be the z-translational mode, based on response in phase and amplitude due to translation of the gravity wheel.

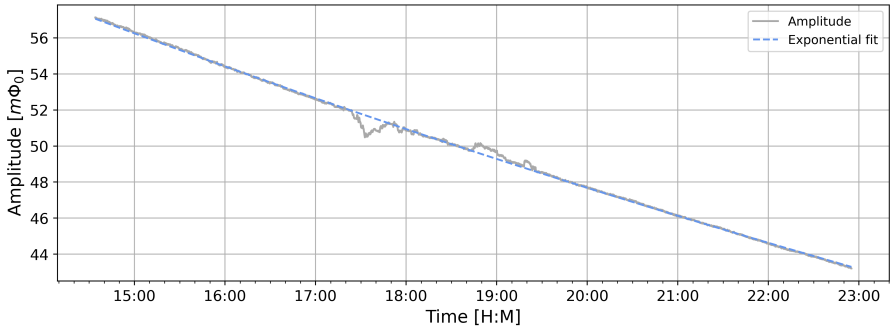


**Fig. B3:** A typical ringdown of the 26 Hz mode, as performed after a magnetic drive through the calibration transformer. The time constant  $\tau$  is extracted from an exponential fit.

The high amplitude  $\tau$  provides a lower bound to the low amplitude  $\tau$  of the system. We observe a significant difference in  $\tau$  for high and low amplitude, which is explained by a duffing non-linearity in the equations of motion of the resonator. From ringdown measurements, we obtain a decay time of  $\tau = 1.09 \cdot 10^5$  s. The error on the fit of this value is 14.7 seconds, however, as we will discuss in a future publication, the decay time of individual modes is partly dependent on the amplitude of other modes due to a coupling of the non-linearities. To avoid this issue in the current publication, we will instead truncate the values at 3 decimals. With the quality factor  $Q$  of the resonator defined as

$$Q = \pi f \tau \quad (\text{B1})$$

with frequency of the mode  $f = 26.7$  Hz, we obtain a quality factor of  $Q = 9.06 \cdot 10^6$ . From  $\tau$  we can also determine the damping coefficient of the resonator, which is defined as

$$\gamma = \frac{2}{\tau} \quad (\text{B2})$$

frequency [Hz]	tau [s]	Q factor
15.9	$3.65 \cdot 10^4$	$1.82 \cdot 10^6$
26.7	$1.09 \cdot 10^5$	$9.13 \cdot 10^6$
40.6	$1.43 \cdot 10^4$	$1.82 \cdot 10^6$
55.1	$3.37 \cdot 10^4$	$5.84 \cdot 10^6$
129	$0.214 \cdot 10^4$	$8.70 \cdot 10^5$
147	$0.152 \cdot 10^4$	$6.98 \cdot 10^5$

**Table B1:** Tabulated values of the resonator mode parameters. Again, these values are truncated at at three decimals, since the fit significance of these values is much higher than the actual stability of these values with respect to mode amplitude, as touched upon in the texts. The spring stiffness of the 26.7 Hz mode was found to be 12.2 mN/m

which gives a damping in the 26 Hz mode of  $\gamma = 1.84 \cdot 10^{-5} \text{ s}^{-1}$ , or a linewidth of  $\gamma/2\pi = 2.92 \text{ } \mu\text{Hz}$

## Appendix C Analysis and Calibration of the Single-Stage Zeppelin Readout Circuit and Energy Coupling, $\beta^2$

The motion of the particle, and the resulting force noise of the particle modes, can be calibrated by injecting a magnetic drive through the calibration transformer. The amount of magnetic flux injected is then directly quantised by the SQUID. By then measuring the flux caused by the particle response, we find an absolute calibration of flux to motion.

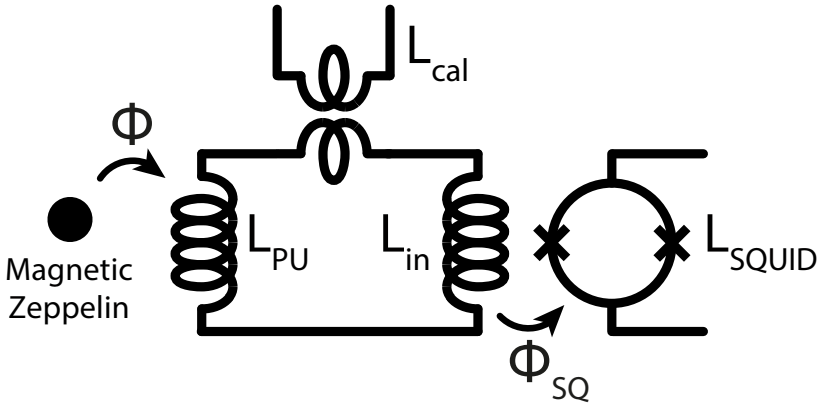


**Fig. C4:** Schematic circuit of the single-stage readout circuit for the magnetic zeppelin.

A simple way of seeing this is from the energy coupling,  $\beta^2$ , defined as the fraction of the energies in two coupled oscillating systems, and can be seen simply as the amount of energy that couples from one system to the other. This is similar to the quality factor of a single system, which is defined as the fraction of energy lost per cycle with respect to the total energy in the system, that is to say, it is a measure for the damping of the system. Conversely, the quality factor also gives a measure for the maximal energy stored in the resonator as a fraction of the input energy when driven at resonance for a time  $T \gg \tau$ , that is to say, the energy at which the fractional energy loss per cycle is equal to the energy put in each cycle by the resonant drive.

For our system, with a mechanical resonator in the form of the trapped zeppelin, and a driving magnetic field coupled in through the calibration transformer and coupled to the zeppelin through the pick-up loop, we get

$$\beta^2 \equiv \frac{L_{total} I^2}{kx^2} \quad (C3)$$

with  $x$  any spatial coordinate. Going to the limit of infinitesimal change in coordinate, and using  $k = m\omega^2$ , we obtain

$$\beta^2 = \frac{\left(\frac{d\Phi}{dx}\right)^2}{L_{total} \cdot m\omega^2} \quad (C4)$$

from which we see that the energy coupling can be used to determine the quantisation of flux measured in the SQUID, to absolute motion of the zeppelin.

To measure  $\beta^2$ , we further consider the motion of the resonator as a simple resonantly driven harmonic oscillator, of the form

$$x(t) = A(t)e^{i\omega t}; \quad A(t) = \frac{F}{2m\omega} \cdot t \quad (C5)$$

from which we obtain a damping force of the form  $F_{damping} (= 2m\zeta\omega_0 \frac{dx}{dt} = \gamma_m v) = \gamma_m \cdot \omega \cdot x$ . Furthermore,  $Q = \frac{1}{2\zeta}$ , thus  $\gamma_m = \frac{m\omega}{Q}$ . When a flux is injected through the calibration transformer, this results in a current through the detection circuit. This current is detected by the SQUID from the resultant flux in the input coil of the SQUID, which is why we refer to this current as the crosstalk current  $I_{crosstalk}$ , but will also result in a flux through the pick-up loop, which gives rise to a magnetic force on the zeppelin of the form  $F_{drive} = \alpha \cdot I_{crosstalk}$  where  $\alpha$  is a coupling constant of units [N/A] that that is partly determined by the geometry. The motion of the zeppelin will in return induce a current in the detection circuit, as a result of the flux change through the pick-up loop, this current has the form  $I_{induced} = \delta \cdot x$  where  $\delta$  is a coupling constant with units [A/m] that is affected by the geometry in the same way as  $\alpha$  is, which can be seen from symmetry. Combining these results, and noting that for the steady state solution the driving force must be equal to the damping force

$$\frac{I_{induced}}{I_{crosstalk}} = \frac{\delta \cdot x}{F_{drive}/\alpha} = \frac{\delta \cdot \alpha \cdot x}{\gamma \cdot \omega \cdot x} = Q \cdot \frac{\alpha \cdot \delta}{m\omega^2} = Q \cdot \frac{\alpha \cdot \delta}{k} \quad (C6)$$

Since some of our  $\tau$  values are rather long, in our experiments we work with a  $Q_{eff} = \pi f T$  where  $T$  is the time during which the drive is applied. From this, we have found that the fraction of the currents in our detection circuit contains all the coupling constants in our system. In fact, looking at the units, we find

$$\frac{\alpha \cdot \delta}{k} = \frac{\left[\frac{\text{N}}{\text{A}}\right] \cdot \left[\frac{\text{A}}{\text{m}}\right]}{\left[\frac{\text{N}}{\text{m}}\right]} \quad (\text{C7})$$

Furthermore, for small displacements in  $x$ , the flux change through the pickup-loop can be treated as linear, which results in the induced current taking the shape  $I_{Induced} = \frac{d\Phi}{dx} \cdot x \cdot \frac{1}{L_{total}}$  or  $\delta = \frac{d\Phi}{dx} \cdot \frac{1}{L_{total}} = \left[\frac{\text{A}}{\text{m}}\right]$ .

As noted before,  $\alpha$  contains the same geometric scaling as  $\delta$ . From the symmetry, we recognise that  $\alpha = \frac{d\Phi}{dx}$  ( $[\text{Wb/m}] = [\text{N/A}]$ ). Combining these results, we find

$$\frac{\alpha \cdot \delta}{k} = \frac{\left(\frac{d\Phi}{dx}\right)^2}{L_{total} \cdot m\omega^2} = \beta^2 \quad (\text{C8})$$

this final results gives us a measurable result for  $\beta^2$ , or, conversely, the proportionality constant  $\frac{d\Phi}{dx}$  that equates our measured flux to an absolute motion. The calibration measure is then found from

$$\frac{d\Phi}{dx} = \sqrt{L_{total} \cdot m\omega^2 \cdot \beta^2} = \sqrt{L_{total} \cdot m\omega^2 \cdot \frac{I_{induced}}{Q \cdot I_{crosstalk}}} \quad (\text{C9})$$

Noting that both  $I_{induced}$  and  $I_{crosstalk}$  are converted equally by the SQUID, the measured voltage can be inserted for the current through the detection circuit, which provides our sensitivity as

$$\frac{d\Phi}{dx} = \sqrt{L_{total} \cdot m\omega^2 \cdot \frac{\Delta V_{drive}}{Q \cdot V_{crosstalk}}} \quad (\text{C10})$$

Here  $\Phi$  is the flux through the pick-up loop. Since we detect this using the SQUID, we need to convert this value to the flux through the SQUID, which is done by dividing by the total inductance of the circuit and multiplying by the mutual inductance of the SQUID input loop and the SQUID loop. As a final step, this value can be related directly to the voltage measures made by taking the SQUID gain value as measured,

$$\frac{dV}{dx} = \frac{dV}{d\Phi_{SQ}} \cdot \frac{d\Phi_{SQ}}{dI} \cdot \frac{dI}{d\Phi} \cdot \frac{d\Phi}{dx} = \frac{dV}{d\Phi_{SQ}} \cdot M_{in,SQ} \cdot \frac{1}{L_{total}} \cdot \frac{d\Phi}{dx} \quad (\text{C11})$$

The values for the inductances in  $L_{total} = L_{PU} + L_{TP} + L_{input} + L_{calibration}$ , are:  $L_{PU} = 2.9 \cdot 10^{-7}$  H the inductance of the pick-up loop,  $L_{TP} = 1 \cdot 10^{-7}$  H the inductance of the 10 cm superconducting twisted-pair connecting the SQUID input to the pick-up loop,  $L_{input} = 4 \cdot 10^{-7}$  H the inductance of the input coil

of the two-stage SQUID device, and  $L_{calibration} = 2 \cdot 10^{-9}$  H the inductance of the small calibration transformer coil. For the mutual inductance, the SQUID is calibrated to a value of  $M_{in,SQ}^{-1} = 0.5 \mu A / \Phi_0$ . The SQUID voltage gain is measured as  $dV/d\Phi_0 = 0.43$ . These values, combined with measures of these ring-up's, gives us a value of  $\frac{dV}{dx} = 0.16 \frac{V}{\mu m}$  for the 26 Hz mode, with a relative error of 7%, which is dominated by the error in the voltage calibration measurement.

## Appendix D Correction and Conversion of the Data to Units of $N/\sqrt{Hz}$

The data used in our gravitational experiments comes from the photodiode detector which measures the passages of the masses on the wheel, and the SQUID signal. Both these signals are filtered by our lock-in amplifiers. Since our gravity experiments were performed at differing amplitudes in the mode, each time trace had a different slope, as discussed in App.B. To account for this, we have subtracted an individual exponential decay in the form of  $Ae^{t/\tau_{fit}}$  from each.

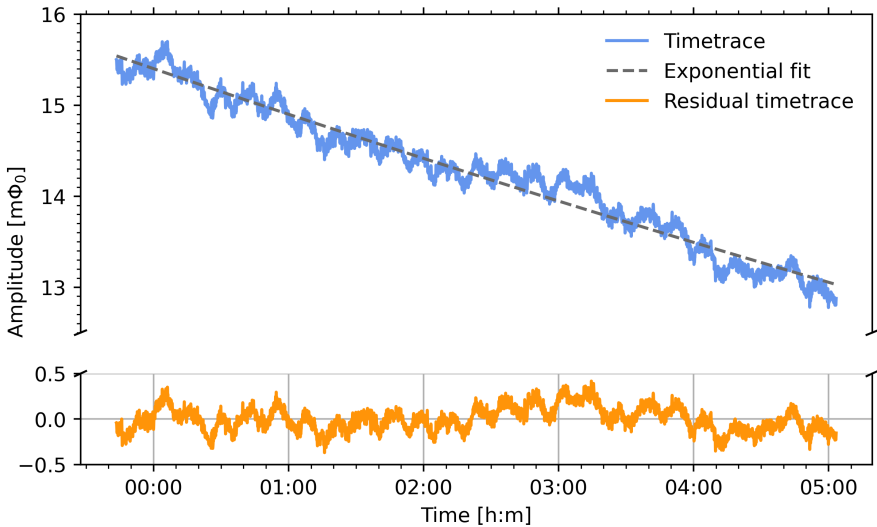


**Fig. D5:** Ringdown subtraction as performed on the time trace measurement of each wheel position. Shown here for a separation between particle and driving mass of 48.1 cm vertical, and laterally displaced by 3.5 cm, when the driving mass is at zero phase. Residual plotted in the lower half, where we see the fluctuations as result of the drive up and drive down effected by the mass-wheel, which is slightly detuned with respect to the mode. We drive detuned since we wish to stay away from the non-linear driving and frequency shift of the mode that happens at large amplitude.

After subtracting the ringdown, we apply a phase factor to the time traces. This phase factor is determined based on the detuning of the zeppelin frequency with respect to the lock-in center frequency. This change ensures that the central peak of the zeppelin will fall fully in a single bin of the Fourier transform we perform next, this ensures that the transfer function of the zeppelin is fully symmetrical. Before performing the Fourier transform, we also cut out a section of the time trace in which there is an integer amount of phase cycles for the mass-passage signal, which ensures smooth periodic boundary conditions for our FFT.

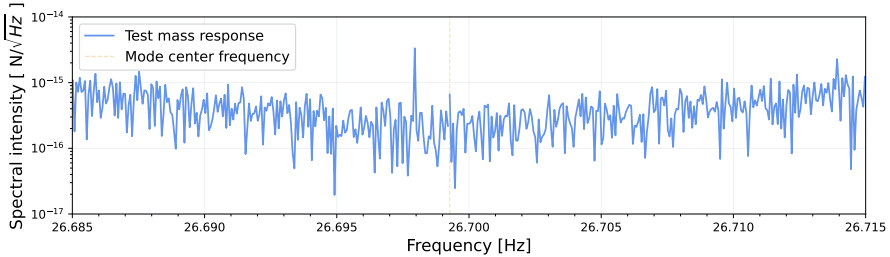


**Fig. D6:** Spectrum of the time trace converted to force noise, the final product of this procedure.

By then subtracting the transfer-function of the mechanical mode from the zeppelin signal, and applying our conversion factor to go from  $\Phi_0$  to displacement, and using a spring stiffness  $k = m\omega^2$  and a mode bandwidth of  $df = Q/f$ , we arrive at our force noise spectrum in  $N/\sqrt{Hz}$

The noise floor of this measurement corresponds to a noise temperature of 3 K, from  $T_{mode} = kx_{RMS}^2/k_B$ .

## References

- [1] Leggett, A.J.: Testing the limits of quantum mechanics: motivation, state of play, prospects **14**(15), 415–451. <https://doi.org/10.1088/0953-8984/14/15/201>. Accessed 2023-03-02
- [2] Arndt, M., Hornberger, K.: Testing the limits of quantum mechanical superpositions **10**(4), 271–277. <https://doi.org/10.1038/nphys2863>. Accessed 2023-03-02
- [3] Disi, L.: Testing spontaneous wave-function collapse models on classical mechanical oscillators **114**(5), 050403. <https://doi.org/10.1103/PhysRevLett.114.050403>. Accessed 2023-03-02
- [4] Vinante, A., Bahrami, M., Bassi, A., Usenko, O., Wijts, G., Oosterkamp, T.: Upper bounds on spontaneous wave-function collapse models

- using millikelvin-cooled nanocantilevers **116**(9), 090402. <https://doi.org/10.1103/PhysRevLett.116.090402>. Accessed 2023-03-02
- [5] Bassi, A., Lochan, K., Satin, S., Singh, T.P., Ulbricht, H.: Models of wave-function collapse, underlying theories, and experimental tests **85**(2), 471–527. <https://doi.org/10.1103/RevModPhys.85.471>. Accessed 2023-03-02
- [6] Ghirardi, G.C., Pearle, P., Rimini, A.: Markov processes in hilbert space and continuous spontaneous localization of systems of identical particles **42**(1), 78–89. <https://doi.org/10.1103/PhysRevA.42.78>. Accessed 2023-03-02
- [7] Disi, L.: A universal master equation for the gravitational violation of quantum mechanics **120**(8), 377–381. [https://doi.org/10.1016/0375-9601\(87\)90681-5](https://doi.org/10.1016/0375-9601(87)90681-5). Accessed 2023-03-02
- [8] Penrose, R.: On gravity’s role in quantum state reduction **28**(5), 581–600. <https://doi.org/10.1007/BF02105068>. Accessed 2023-03-02
- [9] Oosterkamp, T.H., Zaanen, J.: A clock containing a massive object in a superposition of states; what makes Penrosian wavefunction collapse tick? arXiv. <http://arxiv.org/abs/1401.0176> Accessed 2023-03-02
- [10] Westphal, T., Hepach, H., Pfaff, J., Aspelmeyer, M.: Measurement of gravitational coupling between millimetre-sized masses **591**(7849), 225–228. <https://doi.org/10.1038/s41586-021-03250-7>. Accessed 2023-03-02
- [11] Brack, T., Zybach, B., Balabdaoui, F., Kaufmann, S., Palmegiano, F., Tomasina, J.-C., Blunier, S., Scheiwiller, D., Fankhauser, J., Dual, J.: Dynamic measurement of gravitational coupling between resonating beams in the hertz regime **18**(8), 952–957. <https://doi.org/10.1038/s41567-022-01642-8>. Accessed 2023-03-02
- [12] The Lead Zeppelin: a Force Sensor Without a Handle. Casimir PhD Series, vol. 2016-28. Leiden Institute of Physics (LION) , Science , Leiden University. OCLC: 966359873
- [13] Vinante, A., Falferi, P., Gasbarri, G., Setter, A., Timberlake, C., Ulbricht, H.: Ultralow mechanical damping with meissner-levitated ferromagnetic microparticles **13**(6), 064027 1912.12252 [cond-mat, physics:physics, physics:quant-ph]. <https://doi.org/10.1103/PhysRevApplied.13.064027>. Accessed 2023-03-02
- [14] de Wit, M., Welker, G., Heeck, K., Buters, F.M., Eerkens, H.J., Koning, G., van der Meer, H., Bouwmeester, D., Oosterkamp, T.H.: Vibration isolation with high thermal conductance for a cryogen-free dilution refrigerator **90**(1), 015112. <https://doi.org/10.1063/1.5066618>. Accessed



2023-03-02